A new TROPOMI product for tropospheric NO_2 columns over East Asia with explicit aerosol corrections

Mengyao Liu[1#], Jintai Lin[1], Hao Kong[1], K. Folkert Boersma[2,3], Henk Eskes[2], Yugo Kanaya [4], Qin He[5], Xin Tian[6,7], Kai Qin[5], Pinhua Xie[6,7,8], Robert Spurr[9], Ruijing Ni[1], Yingying Yan[10], Hongjian Weng[1], Jingxu Wang[1]

[1]Laboratory for Climate and Ocean-Atmosphere Studies, Department of Atmospheric and Oceanic Sciences, School of Physics, Peking University, Beijing, China

[2]Royal Netherlands Meteorological Institute, De Bilt, the Netherlands

[3]Meteorology and Air Quality department, Wageningen University, Wageningen, the Netherlands

[4]Research Institute for Global Change, Japan Agency for Marine-Earth Science and Technology (JAMSTEC), Yokohama 2360001, Japan

[5]School of Environment and Geoinformatics, China University of Mining and Technology, China University of Mining and Technology, Xuzhou, Jiangsu, 221116, China

[6]Institutes of Physical Science and Information Technology, Anhui University, Hefei, 230601, China

[7]Key laboratory of Environmental Optical and Technology, Anhui Institute of Optics and Fine Mechanics, Chinese Academy of Science, Hefei, 230031, China

[8]CAS Center for Excellence in Urban Atmospheric Environment, Institute of Urban Environment, Chinese Academy of Sciences, Xiamen 361021, China

[9]RT Solutions Inc., Cambridge, Massachusetts 02138, USA

[10]Department of Atmospheric Sciences, School of Environmental Studies, China University of Geosciences (Wuhan), Wuhan, China

Correspondence to: Jintai Lin (linjt@pku.edu.cn)

Now at Royal Netherlands Meteorological Institute (KNMI)

Abstract

We present a new product with explicit aerosol corrections, POMINO-TROPOMI, for tropospheric nitrogen dioxide (NO_2) vertical column densities (VCDs) over East Asia, based on the newly launched TROPOspheric Monitoring Instrument with an unprecedented high horizontal resolution. Compared to the official TM5-MP-DOMINO (OFFLINE) product, POMINO-TROPOMI shows stronger concentration gradients near emission source locations and better agrees with MAX-DOAS measurements (R^2 = 0.75, NMB = 0.8% versus R^2 = 0.68, NMB =

− 41.9%). Sensitivity tests suggest that implicit aerosol corrections, as in TM5-MP-DOMINO, lead to underestimations of NO_2 columns by about 25% over the polluted Northern East China region. Reducing the horizontal resolution of a priori NO_2 profiles would underestimate the retrieved NO_2 columns over isolated city clusters in western China by 35% but with overestimates by more than 50% over many offshore coastal areas. The effect of a priori NO_2 profiles is more important under calm conditions.

1 Introduction

Nitrogen oxides ($NOx = NO + NO_2$) are crucial gaseous pollutants in the troposphere. NOx lead to the production of particulate matter and ozone (O_3) and enhance levels of oxidants in the troposphere (Shindell et al., 2009), which affect air quality (Dentener et al., 2003) and human health (Hoek et al., 2013). Satellite remote sensing is widely used to monitor levels of nitrogen dioxide (NO_2) pollution worldwide (Krotkov et al., 2016; Lin et al., 2010; McLinden et al., 2014; Ott et al., 2010; Russell et al., 2011). The TROPOspheric Monitoring Instrument (TROPOMI), which was jointly developed by the Netherlands and Europe Space Agency (ESA) (Veefkind et al., 2012) and was launched on October 13th 2017, is a UV/Visible/Near-Infrared/Short-wave infrared backscattering sensor onboard the sun-synchronous Sentinel-5 Precursor (S5P) satellite with an overpass time of 13:30 local solar time. With a wide swath of 2,600 km and an unprecedentedly high horizontal resolution of 3.5×7 km^2, (3.5 x 5.5 km^2 since 6 August 2019) TROPOMI achieves daily global coverage. This high horizontal resolution and good spatial coverage, combined with the very high signal-to-noise ratio, enables the instrument to resolve NO_2 pollution from point sources, medium-size urban centers, highways or rivers, tasks that were difficult to achieve before.

Retrievals of tropospheric NO_2 vertical column densities (VCDs) in the UV/Vis spectral range from satellite instruments consist of three steps: (1) using the Differential Optical Absorption Spectroscopy (DOAS) to fit the slant column density (SCD) of NO_2 along the light path, (2) subtracting the stratospheric contribution from the SCD to obtain the tropospheric SCD, and (3) converting the tropospheric SCD to the tropospheric VCD by using the calculated air mass factor (AMF). For TROPOMI, the random uncertainty of the total SCDs is ~ 0.6×10^{15} molec·cm^{-2}, considerably smaller than for the Ozone Monitoring Instrument (OMI, ~ 0.8×10^{15} molec·cm^{-2}, (Zara et al., 2018)). The (total or stratospheric) bias is generally between 0 and -10% according to SAOZ observations (Eskes et al., 2019), which meets the error requirements as defined in the S5P Calibration and Validation Plan (Goryl et al., 2017). The calculation of the AMF introduces the dominant source of error in the retrieved tropospheric NO_2 VCDs over polluted areas (Boersma et al., 2004; Boersma et al., 2011; Boersma et al., 2018; Lin et al., 2014; Lorente et al., 2017). The median negative biases of the daily comparisons between tropospheric VCDs from the Dutch official TM5-MP-DOMINO (OFFLINE) product and MAX-DOAS measurements are generally less than 50% (the allowable bias is 25-50% (Goryl et al., 2017)) but quite variable with the stations and NO_2 levels, especially at polluted locations (Eskes et al., 2018; van Geffen, Eskes, Boersma, Maasakkers et al., 2019).

TM5-MP-DOMINO uses implicit aerosol corrections by assuming aerosols to be "effective clouds", as assumed in most satellite NO_2 products except POMINO (J. T. Lin et al., 2015; J. T. Lin et al., 2014; Liu et al., 2019). In addition, TM5-MP-DOMINO employs a priori NO_2 profiles from the TM5 model at a relatively coarse horizontal resolution (1° × 1°) (Williams, Boersma, Le Sager, & Verstraeten, 2017). The implicit aerosol corrections (Lin et al., 2014; Liu et al., 2019; Lorente et al., 2017) and the coarse horizontal resolution of a priori NO_2 profile data (Laughner, Zare, & Cohen, 2016; McLinden et al., 2014; Russell et al., 2011) may be the largest sources of the large biases observed between TM5-MP-DOMINO and MAX-DOAS. Based on previous studies for OMI, implicit aerosol corrections can lead to more than 50% uncertainties over polluted areas with high aerosol loadings like China (Lin et al., 2014; Liu et al., 2019; Lorente et al., 2017). Eskes et al. (2018) showed that using a priori NO_2 profiles from the regional CAMS model at a 12 × 12 km^2 resolution to replace the TM5 NO_2 profiles increase the retrieved NO_2 VCDs by ~0 to 50% over Western Europe depending on the location.

Here we present a new TROPOMI tropospheric NO_2 VCD product over East Asia, namely POMINO-TROPOMI. This product is based on our POMINO algorithm (Lin et al., 2015; Lin et al., 2014; Liu et al., 2019) previously applied to OMI. POMINO-TROPOMI improves upon TM5-MP-DOMINO by employing explicit aerosol corrections and using high-resolution (~25 km) a priori NO_2 profiles, among other improvements. POMINO-TROPOMI NO_2 VCD data over July-October 2018 are presented and validated by MAX-DOAS measurements, along with additional sensitivity tests of the effects of aerosol representations and a priori NO_2 profiles.

2 Method and Data

2.1 POMINO-TROPOMI retrieval algorithm and product

As one of the UV/Vis backscatter instruments to observe NO_2, TROPOMI inherits much of the design of OMI (Veefkind et al., 2012). Thus the POMINO-TROPOMI algorithm here largely follows our previous POMINO algorithm (Liu et al. (2019)), with some modifications to adapt to its high horizontal resolution and different cloud retrieval procedure.

The POMINO-TROPOMI algorithm focuses on improving the calculation of tropospheric AMF. It thus takes the tropospheric SCD data from TM5-MP-DOMINO (OFFLINE), which are obtained by fitting the 405-465 nm wavelength range with the DOAS method. Our tropospheric AMF calculation is done for 437.5 nm, following TM5-MP-DOMINO.

We use the parallelized LIDORT-driven AMFv6 package to derive tropospheric AMFs via online pixel-specific radiative transfer calculations, with no use of look-up tables. Our algorithm explicitly accounts for aerosol optical effects and anisotropic properties of surface reflectance, uses daily a priori aerosol and NO_2 profiles from the simulation of nested GEOS-Chem model (0.25° lat. × 0.3125° long.), and further uses Aerosol Optical Depth (AOD) data from Moderate Resolution Imaging Spectroradiometer (MODIS/Aqua) to correct GEOS-Chem simulated aerosols on a monthly basis. Figure 1 shows the procedure of using the AMFv6 package to derive the tropospheric NO_2 VCDs of POMINO-TROPOMI. Table S1 shows the retrieval parameters in POMINO-TROPOMI, in comparison with those in TM5-MP-DOMINO and POMINO v2.

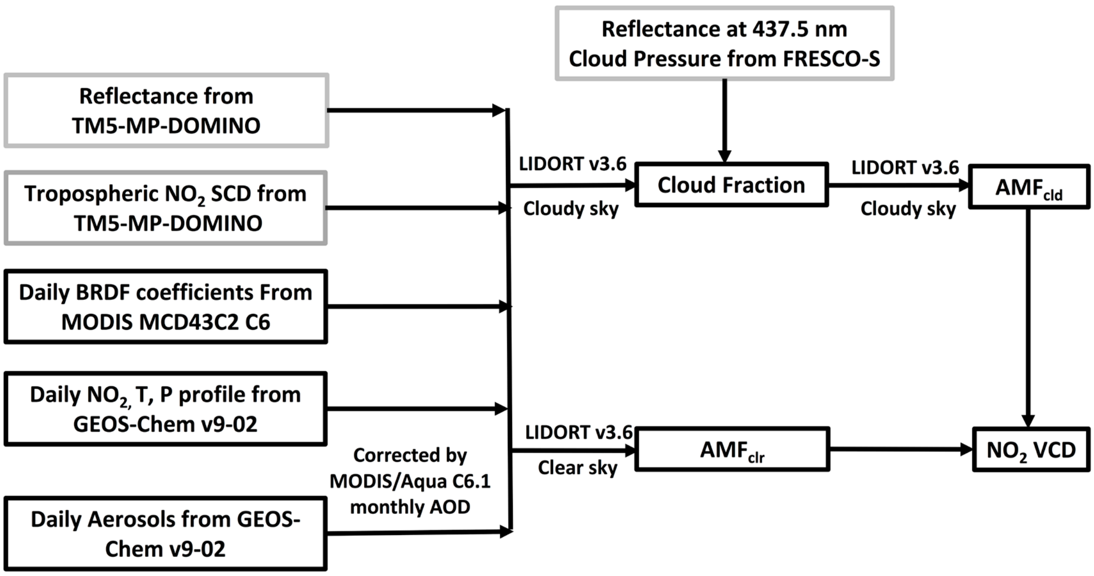

Figure 1. Flowchart of the POMINO-TROPOMI algorithm. The grey rectangles represent the parameters from the TM5-MP-DOMINO (OFFLINE) product.

The independent pixel approximation (IPA) is used to calculate AMF as a linear combination of a cloudy AMF (M_{cld}) and a clear-sky AMF (M_{clr}):

$$M = wM_{\mathrm{cld}} + (1 - w)M_{\mathrm{clr}} \quad (1)$$

w is the cloud radiation fraction (CRF) calculated by:

$$w = \frac{f_{\mathrm{eff}} I_{\mathrm{cld}}}{R} = \frac{f_{\mathrm{eff}} I_{\mathrm{cld}}}{f_{\mathrm{eff}} I_{\mathrm{cld}} + (1 - f_{\mathrm{eff}}) I_{\mathrm{clr}}} \quad (2)$$

where I_{cld} denotes the radiance from the cloudy part of the pixel, I_{clr} the radiance from the clear-sky part of the pixel, f_{eff} the cloud fraction (CF), and the R the total scene radiance. Retrieval of cloud properties is a prerequisite for NO_2 retrieval. We take the effective cloud pressure (CP) from the FRESCO-S algorithm (van Geffen et al., 2019) which uses the O_2 A-band (around 758 nm) for TROPOMI trace gas retrievals. We re-calculate w and f_{eff} at the NO_2 fitting wavelength (437.5 nm). The online CF calculation is similar to that for TM5-MP-DOMINO (Arnoud et al., (2017); van Geffen et al., 2019), but with an explicit aerosol correction to be consistent with the following NO_2 retrieval and to remove the aerosol signal from the retrieved CF data.

For explicit aerosol corrections in this study, we take daily aerosol simulation results from the GEOS-Chem v9-02 nested model over East Asia, followed by a monthly AOD correction using MODIS/Aqua C6.1 AOD data. Our future study will use the CALIOP aerosol extinction vertical profiles to further improve the modeled aerosol profiles. Figure 2b shows the spatial distribution of AOD in July 2018 used in clouds and NO_2 retrievals. The AOD distribution is consistent ($R = 0.42$, $N = 1447$) with that of near-surface $PM_{2.5}$ mass concentration measurements (Fig. 2a) taken from the Ministry of Ecology and Environment of China (MEE); the difference between AOD and near surface $PM_{2.5}$ is expected because they represent different parameters of aerosols.

The criteria to select valid pixels in this study are as follows. We exclude pixels with viewing zenith angles (VZAs) greater than 80°, with high albedos caused by ice or snow on the ground, or with quality flag (from TM5-MP-DOMINO) less than 0.5. To screen out cloudy scenes, we discard pixels with CRFs greater than 50% in the POMINO-TROPOMI product.

In addition to our formal POMINO-TROPOMI product (referred to as Case REF), we use sensitivity cases to evaluate the impacts of aerosol corrections (explicit versus implicit) and the horizontal resolution of a priori NO_2 profiles (Cases 1 and 2 in Table 2). Two additional cases (Cases 3 and 4) concern the treatment of CP in combination with the choice of aerosols and surface reflectance. Specifically, using the CP data directly from FRESCO-S means that our retrieval algorithm does not perfectly account for the effect of aerosols on clouds. Our retrieval consider the BRDF effects while Lambertian surface is used in deriving the FRESCO-S CP. To ensure sampling consistency, the pixels used in all cases are selected based on the CRF values in Case REF.

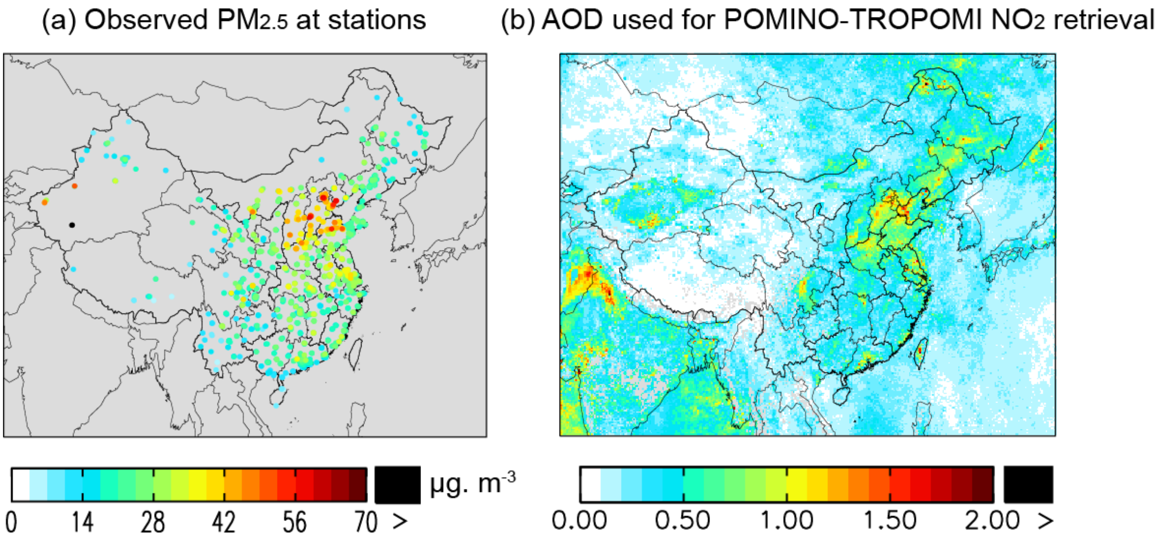

Figure 2. (a) Observed near-surface $PM_{2.5}$ mass concentrations averaged over July 2018. Results are sampled at the times of valid TROPOMI data. (b) AOD data on a 0.05° × 0.05° grid used for the retrieval of POMINO-TROPOMI NO_2 VCDs in July 2018.

2.2 Ground-based MAX-DOAS measurements

We use ground-based MAX-DOAS measurements to validate the POMINO-TROPOMI NO_2 product. The MAX-DOAS measurements are from two suburban stations (Xuzhou and Nanjing) and one remote station (Fukue, (Kanaya et al., 2014)). Table 1 shows the geographical and time information of each MAX-DOAS site, and SI Part A describes each instrument in detail. Although Xuzhou and Nanjing are both classified as suburban sites located at university campuses, the NO_2 spatial distributions around the two sites are very different. The spatial distribution of NO_2 VCDs is relatively smooth around Xuzhou, whereas the VCDs exhibit a strong spatial gradient around Nanjing (Figure 3).

A consistent spatiotemporal sampling is crucial in comparing satellite measurements and MAX-DOAS data (Boersma et al., 2018; Lin et al., 2014; Liu et al., 2019; Wang et al., 2017). We average all valid MAX-DOAS data within ±1 hours of the TROPOMI overpass time to obtain daily values for comparison. To reduce the influence of local events, we exclude all MAX-DOAS data whose standard deviations within the two hours exceed 20% of their mean values. We average all valid pixels within 5 km of each MAX-DOAS site to represent the respective daily satellite data. SI Part B shows how the validation results are affected by the sampling choice.

Table 1. MAX-DOAS measurement sites.

Site name	Geographical location	Measurement time
Nanjing	118.950° E, 32.118° N, 36 m	2018/07/01-2018/10/31
Xuzhou	117.142° E, 34.217° N, 92 m	2018/07/01-2018/10/31
Fukue	128.680° E, 32.750° N, 83 m	2018/07/01-2018/09/15

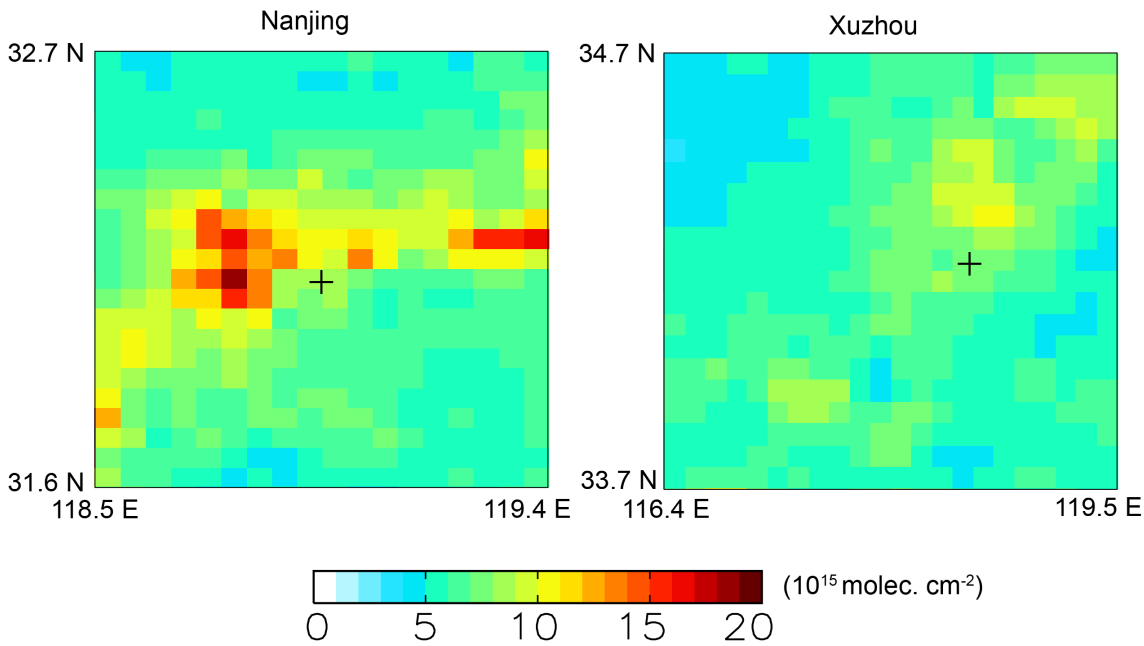

Figure 3. Spatial distributions of POMINO-TROPOMI NO_2 VCDs (on a 0.05° × 0.05° grid) around (a) Nanjing and (b) Xuzhou MAX-DOAS measurement sites in July 2018. The MAX-DOAS sites are marked as "+".

3 Results

3.1 POMINO-TROPOMI NO_2 VCDs over East Asia

Figure 4b shows the spatial distribution of POMINO-TROPOMI tropospheric NO_2 VCDs over East Asia on a 0.05° × 0.05° grid in July 2018. High VCD values (> 3 × 10^{15} molec. cm^{-2}) are shown over polluted areas such as East China and India, and low values (< 1 × 10^{15} molec. cm^{-2}) over the open ocean and the Tibetan Plateau. For comparison, the colored dots in Fig. 4a visualize the near-surface NO_2 concentrations observed at the MEE sites at the overpass time of TROPOMI. In both the VCD and the near-surface concentration maps (Fig. 4a and b), hotspots like urban centers and isolated sources can be seen clearly, due to the short lifetimes of NO_X in summer. The spatial correlation is about 0.55 (N = 1458) between the VCD and the near-surface concentration distributions.

Figure 4c shows the spatial distribution of TM5-MP-DOMINO (OFFLINE) NO_2 VCDs for comparison. The general distribution of TM5-MP-DOMINO is consistent with that of POMINO-TROPOMI with a correlation coefficient of 0.97 (N = 1091154). However, TM5-MP-DOMINO NO_2 VCD values are lower than POMINO-TROPOMI by about 35% averaged over the whole domain (Fig. 4d), by −37 − 68% over cleaner areas (POMINO-TROPOMI < 5 × 10^{15} molec. cm^{-2}), and by 0 − 66% over more polluted areas (POMINO-TROPOMI ⩾ 5 × 10^{15} molec. cm^{-2}). TM5-MP-DOMINO does not show strong local signals at pollution hotspots like the urban center of Beijing (Fig. 4c). Over these hotspot locations, TM5-MP-DOMINO is lower than POMINO-TROPOMI by up to 5 × 10^{15} molec. cm^{-2}.

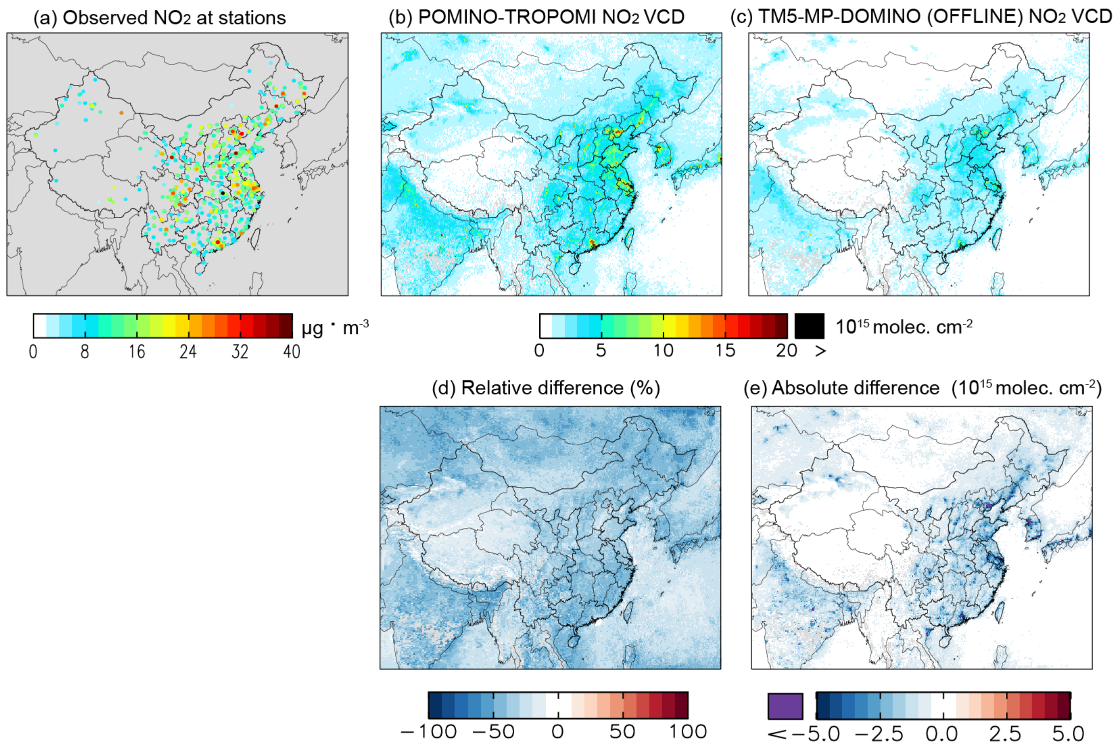

Figure 4. The spatial distribution of (a) NO_2 at monitoring stations, (b) AMFv6 derived NO_2 VCD and (c) TM5-MP-DOMINO (OFFLINE) NO_2 VCD at 0.05° × 0.05° grid in July 2018. (d) and (e) are relative and absolute difference of TM5-MP-DOMINO (OFFLINE) to POMINO-TROPOMI NO_2 VCD.

Table 2. Sensitivity experiments for the NO_2 retrieval based on the POMINO-TROPOMI algorithm.

ID	A priori NO_2 profiles	Aerosols	Surface reflectance
Case REF (POMINO-TROPOMI)	0.25° lat. × 0.3125° long.	Explicit	MODIS BRDF
Case 1	Same as Case REF	N/A	Same as Case REF
Case 2	2° lat. × 2.5° long.	N/A	Same as Case REF
Case 3	Same as Case REF	Semi-explicit [1]	Same as Case REF
Case 4	Same as Case REF	Same as Case REF	OMI LER [2]

[1] Explicit aerosol treatments for M_{clr} and no aerosol corrections for M_{cld}.

[2] The LER dataset is a five-year climatology built upon OMI measurements on a grid of 0.5° × 0.5°. The dataset is taken from the TM5-MP-DOMINO product.

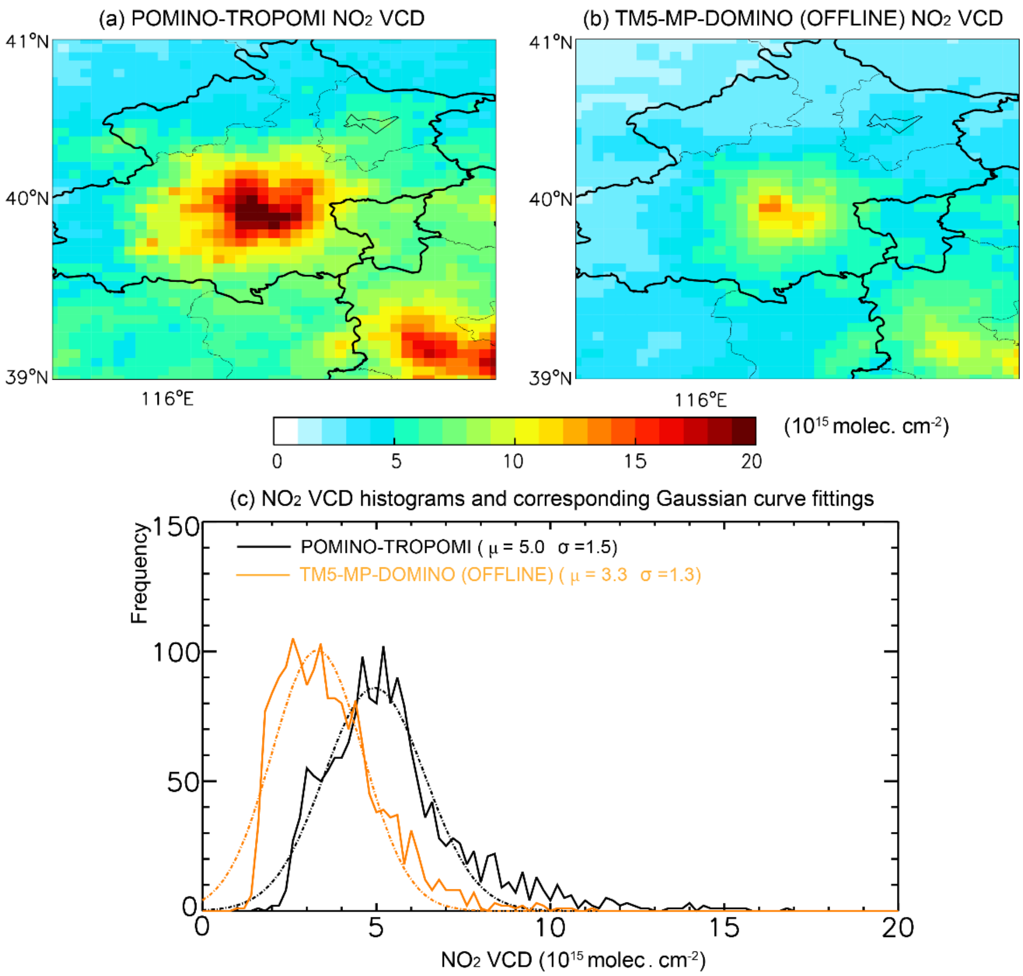

Figure 5. Spatial distributions of (a) POMINO-TROPOMI NO_2 VCDs and (b) TM5-MP-DOMINO (OFFLINE) NO_2 VCDs on a 0.05° × 0.05° grid over Beijing and its surrounding areas averaged over July 2018. (c) Histograms of monthly NO_2 VCDs over this region. The bin size is 0.2×10^{15} molec·cm^{-2}. The black and orange dashed lines are corresponding Gaussian curve fitting of the histograms. μ is the mean value and σ is the standard deviation of a Gaussian curve fitting.

Figure 5a and b present the two products over Beijing and surrounding areas, showing a much weaker spatial gradient of NO_2 VCDs from Beijing urban center to its outskirts in TM5-MP-DOMINO than in POMINO-TROPOMI. The corresponding histograms and Gaussian fittings in Fig. 5c also show a lower mean value and a smaller standard deviation of TM5-MP-DOMINO than POMINO-TROPOMI. These results highlight the important differences between the two products at fine scales.

We further compare the two satellite products with ground-based MAX-DOAS measurements at three sites. The scatter plots in Fig. 6a and b compare the NO_2 VCDs on 63 days (from 109 pixels) over July–October 2018 with their MAX-DOAS counterparts. Different colors differentiate the sites. POMINO-TROPOMI captures the day-to-day variability in MAX-DOAS data (R^2 = 0.75) and shows a small normalized mean bias (NMB = 0.8%). The reduced major axis (RMA) regression shows a slope of 0.70, mainly because of the underestimate on high-NO_2 days. TM5-MP-DOMINO is also correlated with MAX-DOAS (R^2 = 0.68), although the correlation is weaker than our retrieval. The NMB of TM5-MP-DOMINO is much more significant (−41.9%) and the RMA regression slope is much smaller (0.42). Similar underestimates of TM5-MP-DOMINO have been discussed in their Readme document (Eskes et al., 2019) and ATBD file (van Geffen et al., 2019) in general, in Griffin et al. (2019) for Canada. Major plausible causes of the underestimate of TM5-MP-DOMINO include coarse-resolution climatological surface albedo data, coarse-resolution (1° × 1°) a priori NO_2 profiles, implicit aerosol corrections, and uncertainties of CP from FRESCO-S.

Cloud pressures from FRESCO-S are found to be too high, i.e., the cloud top is too close to the ground, especially over China (van Geffen et al., 2019). We examine this effect by excluding the pixels with CP > 850 hPa when comparing with MAX-DOAS data. With this additional criterion, the number of valid days drop to 20. Figure 6c and d show the scatter plots and corresponding RMA results. The NMB of TM5-MP-DOMINO is reduced slightly to -38.2%, and its R^2 for day-to-day variation is increased from 0.68 to 0.85. POMINO-TROPOMI still outperforms TM5-MP-DOMINO: 0.85 versus 0.85 for R^2, 13.8% versus -38.2% for NMB, and 0.82 versus 0.56 for RMA regression slope. The improvement from excluding CP > 850 hPa scenes is larger in TM5-MP-DOMINO (with implicit aerosol corrections) than in POMINO-TROPOMI (with explicit aerosol corrections). The averaged CF of data excluding CP > 850 hPa is 0.13 (AOD = 0.63), which is much larger than the averaged value (CF = 0.06) in Fig. 6a and b (AOD = 0.57). This appears to imply that the overestimated CP be partly because the FRESCO-S cloud algorithm might mis-interpret heavy aerosol loadings near the ground as clouds, a common issue in satellite data (Lin & Li, 2016).

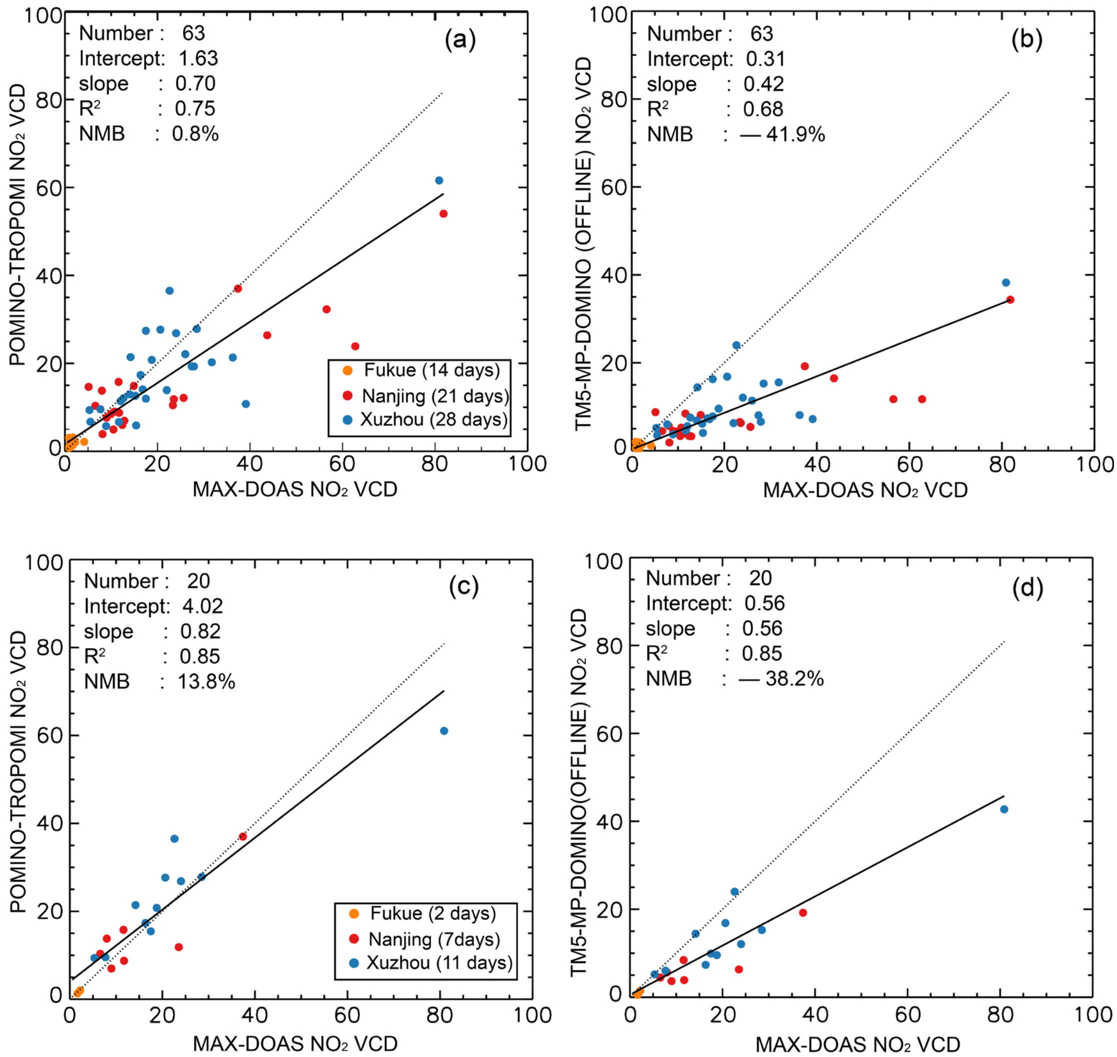

Figure 6. Scatter plot for daily NO_2 VCDs (10^{15} molec·cm^{-2}) between MAX-DOAS and two TROPOMI NO_2 VCD products. Each colored dot represents a day and each color denotes a station. For each day, the satellite data are averaged over all pixels. (c) and (d) are results for the two TROPOMI NO_2 VCD products with effective cloud pressures $\leq$ 850 hpa.

3.2 Influences of aerosol correction approaches and horizontal resolutions of a priori NO_2 profiles

To investigate the causes of difference between POMINO-TROPOMI and TM5-MP-DOMINO (OFFLINE), we conduct two sensitivity retrievals based on the POMINO-TROPOMI algorithm (Cases 1 and 2 in Table 2). Figure 7 shows the relative (a−c) and absolute (d−f) differences between retrieval cases (REF, Case 1 and Case 2). Case 1 adopts the implicit aerosol correction for both clouds and NO_2 retrievals, as in TM5-MP-DOMINO, so the difference between REF and Case 1 indicates the effect of aerosol representation (explicit versus implicit) (Fig. 7a, d). In Case 2, the high-resolution (0.25° lat. × 0.3125° long.) NO_2 profiles are replaced by low-resolution (2° lat. × 2.5° long.) profiles simulated by the GEOS-Chem global model; aerosols are represented implicitly as in Case 1. Case 2 thus mimics TM5-MP-DOMINO, which uses an implicit aerosol correction and coarse-resolution NO_2 profiles. Thus, the difference between Case 1 and Case 2 arises from the a priori NO_2 profiles (Fig. 7b, e). The difference between Case 2 and REF further indicates the joint effect of using coarse-resolution a priori NO_2 profiles and an implicit aerosol correction (Fig. 7c, f).

Figure 7 shows that the individual influences of aerosol representations (explicit versus implicit) and a priori NO_2 profiles (fine versus coarse resolution) vary substantially from one location to another. The impacts of aerosol corrections are most evident over the areas of heavy aerosol loadings including East China, India and parts of Southeast Asia. The implicit aerosol correction (Case 1) tends to result in lower NO_2 VCDs by 0-50% over urban areas compared to the explicit aerosol correction (Case REF) (Fig. 7a, d). By comparison, the impacts of NO_2 profiles are spatially more heterogeneous (Fig. 7b and e). Over the offshore coastal areas, using coarse-resolution NO_2 profiles (Case 2) tends to overestimate the NO_2 VCDs by 30-100% relative to when high-resolution profiles are used (Case 1), due to overly (horizontal) smoothing of NO_2.

Below, we discuss these differences over two key areas including Northern East China and Xinjiang. Northern Eastern China (bounded by the black rectangle in Fig. 4a) is a heavy aerosol-loaded region (Fig. 2). Over this region, an implicit rather than explicit aerosol representation results in lower NO_2 VCDs by ~25% (Fig. 7a, d), while the effect of NO_2 profiles is weaker (Fig. 7b, e). The joint effect is dominated by the effect of aerosol representation (Fig. 7c, f).

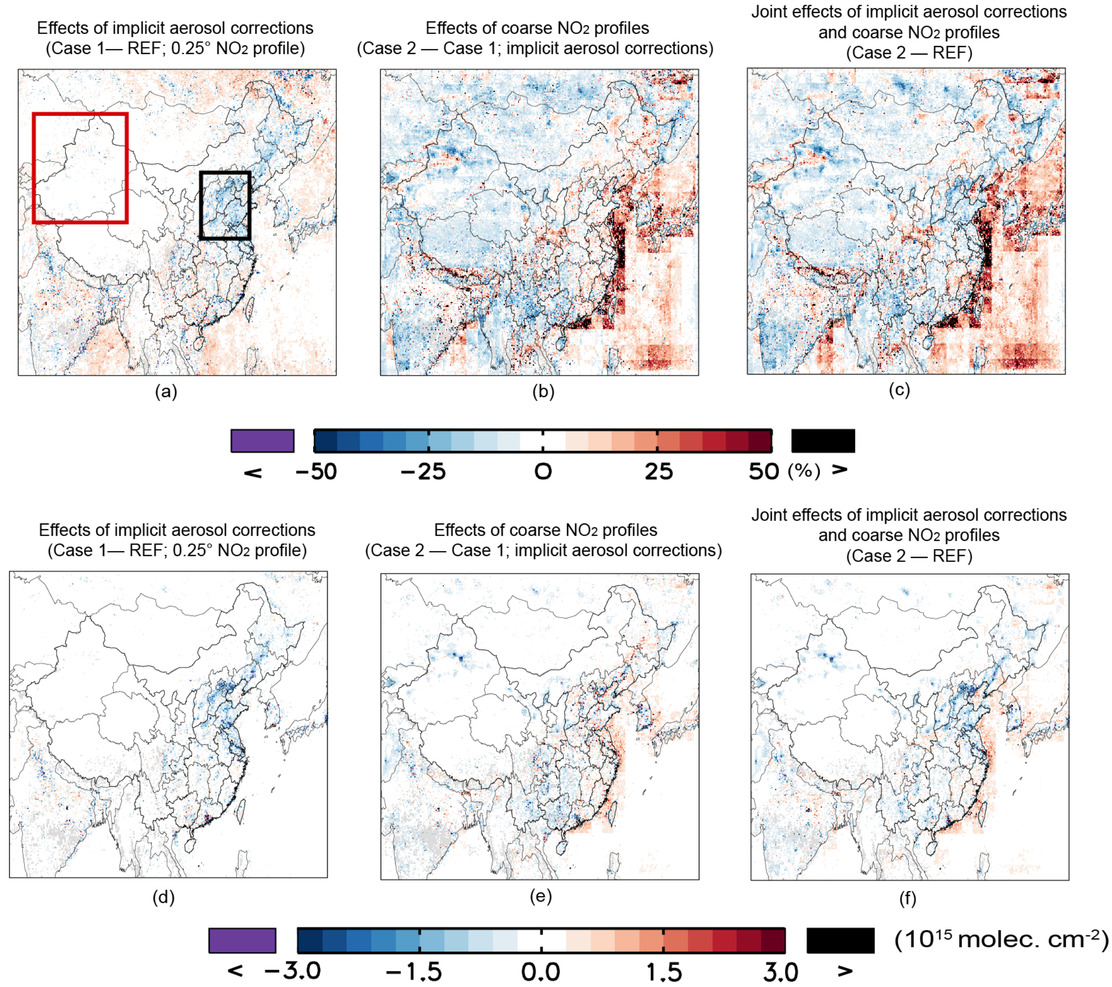

Figure 7. (a)−(c) Relative differences caused by aerosol corrections and a priori NO_2 profiles. (d)−(f) are the corresponding absolute differences. The black and red rectangles stand for Northern Eastern China and Xinjiang, respectively.

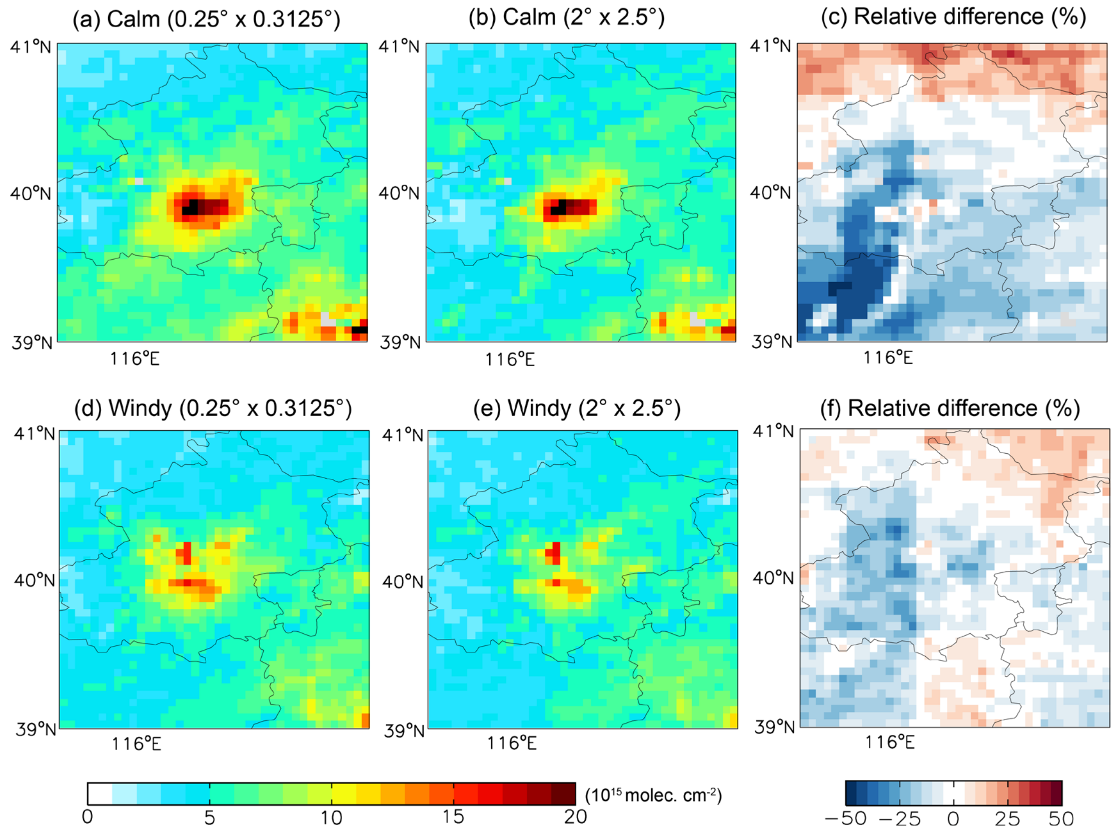

Figure 8. Spatial distributions of POMINO-TROPOMI NO_2 VCDs on a 0.05° × 0.05° grid under calm conditions with (a) 0.25° lat. × 0.3125° long. NO_2 profiles (Case 1), with (b) 2° lat. × 2.5° long. profiles (Case 2), and (c) their relative differences. (d)−(f) is similar to (a)−(c) but under southward wind.

That the impact of a priori NO_2 profiles is relatively small over Northern Eastern China is partly because of the smearing effect by wind. Figure 8 differentiates the effects of NO_2 profiles between twenty-three windy (daily average wind speed under 500 m > 2 m s^{-1}) days and seven calm (wind speed < 2 m s^{-1}) days. The dataset of wind is taken from National Aeronautics and Space Administration/Global Modeling and Assimilation Office’s (NASA/GMAO's) “forward-processing” (GEOS-FP) data product with the horizontal resolution at 0.25° lat. × 0.3125° long. In the windy cases, the NO_2 VCDs are much more smoothed even at 0.3125° resolution, thus the difference of NO_2 resolutions is very small. In contrast, NO_2 VCDs exhibit much stronger horizontal gradient in calm situations, which are better retrieved when high-resolution NO_2 profile are used. As calm situation is more favorable for pollutant accumulation while windy days help to dilute concentration of NO_2, so much higher NO_2 VCDs are found in Fig. 8a and b.

Xinjiang (bounded by the red rectangle in Fig. 7a) is a deserted region in West China. Over Xinjiang, the resolution of a priori NO_2 profiles affects the retrieved NO_2 VCDs much more than the aerosol representation does (Fig. 7b and e). Compared to Case 1 (with high-resolution NO_2 profiles), Case 2 (with coarse-resolution profiles) leads to much lower NO_2 VCDs over the isolated urban areas which are not resolved by the coarse model.

3.3 Influences of directly using the CP data from FRESCO-S

As we take the CP data directly from the FRESCO-S retrieval rather than re-retrieving CP (as done for CF), two main issues arise. First, the FRESCO-S retrieved CP may be affected by aerosols, thus using such CP data in our explicit aerosol corrections (Case REF) may lead to over-correction of aerosol effects. To estimate the effect of such over-correction on retrieved NO_2 VCDs, we employ in an additional sensitivity case (Case 3 in Table 2) a “semi-explicit” aerosol correction approach. This approach explicitly includes aerosols in the calculation of AMF for the clear-sky portion (M_{clr}) of a pixel (as in Case REF), but excludes aerosols for the cloudy-sky portion (M_{cld}) of that pixel. Correspondingly, CF is re-calculated on the basis that the radiance at 437.5 nm received by TROPOMI is contributed from the aerosol-contained clear-sky portion and the no-aerosol cloudy-sky portion. Table 3 shows that in July 2018, on a pixel basis, the derived NO_2 in Case 3 are larger than those in Case REF, with an average difference increasing from 3.1% at relatively clean situations (NO_2 VCDs in Case REF < 5×10^{15} molecu· cm^{-2}) to 11.2% for polluted situations (NO_2 VCDs in Case REF ≥ 15×10^{15} molecu· cm^{-2}). The spatial distributions in Fig. S1a and S1b also show higher NO_2 VCDs in Case 3 relative to Case REF. The corresponding increases in CF (Fig. S1c versus S1d) are because in Case 3 the scattering contributions to the radiance from aerosols in the cloudy-sky portion (that would have occurred) are accounted for with higher CFs. The enhanced “shielding effect” of clouds (due to higher CFs) result in lower NO_2 AMFs and higher VCDs.

For surface reflectance, Case REF considers the BRDF effect instead of Lambertian Equivalent Reflectivity (LER) which is used in deriving FRESCO-S clouds. This leads to inconsistency between when the CP is derived and when it is used. The LER data used by FRESCO-S are generated at 758 and 772 nm (based on the Global Ozone Monitoring Experiment-2), rather than at the 437.5 nm for the NO_2 retrieval. Thus Case 4 adopts the OMI LER data from TM5-MP-DOMINO, a five-year monthly based climatology at 440 nm, and re-calculates CFs and NO_2 AMFs with explicit aerosol corrections and FRESCO-S CP (Table 2). Here, the ice-snow flag in the TM5-MP-DOMINO product is used to exclude the possible ice/snow contamination, and only the pixels with blue-sky albedos (derived from the BRDF data in Case REF) less than 0.3 are taken into consideration. The resulting NO_2 VCDs in Case 4 are lower than Case REF by 3.7% on pixel-based average for relatively clean situations and by 8.3% for polluted situations (Table 3). Figure S2a and S2b further shows the spatial distributions of the relative and absolute differences in derived monthly mean NO_2 VCDs between Case 4 and Case REF. In general, Case 4 leads to lower NO_2 VCDs than Case REF because of stronger surface reflectance, as is obvious in the comparison of blue-sky albedo in Case REF and LER albedo in Case 4 (Fig. S2c versus S2d).

Table 3. Effects of choices of aerosols and surface reflectance inconsistent with using the CP data from FRESCO-S in July 2018.

Situation [1]	Effect of aerosol correction choice (Case 3 – REF) [2]	Effect of surface reflectance choice (Case 4 – REF) [2]
NO_2 VCD < 5×10^{15} molecu$\cdot$ cm^{-2} Mean AOD: 0.27 Mean CF: 0.07 Mean CP: 748 hPa	3.1%	−3.7%
5×10^{15} molecu$\cdot$ cm^{-2} $\leqslant$ NO_2 VCD < 15×10^{15} molecu$\cdot$ cm^{-2} Mean AOD: 0.65 Mean CF: 0.08 Mean CP: 767 hPa	4.1%	−8.1%
15×10^{15} molecu$\cdot$ cm^{-2} $\leqslant$ NO_2 VCD Mean AOD: 0.66 Mean CF: 0.09 Mean CP: 772 hPa	11.2%	−8.3%

[1] The values of AOD, CF and CP shown here are mean values of the pixels of corresponding subsets in Case REF.

[2] The percentage values represent the mean relative differences relative to Case REF.

3.4 Error estimates for POMINO-TROPOMI NO_2 AMFs

It is difficult to derive an overall AMF error for each pixel with our algorithm, particularly because of the three-dimensional aerosol parameters used, the inter-linkage between clouds and other parameters (aerosols and surface reflectance), and the exclusion of LUTs (which leads to too computationally expensive error estimates). Table 4 provides a preliminary estimate of the NO_2 AMF errors with respect to uncertainties in individual parameters. We follow the ATBD of TM5-MP-DOMINO (van Geffen et al., 2019) and make use of error estimates in previous studies. Individual errors with respect to CF, CP and BRDF coefficients are within 10%. Errors with respect to aerosols are considered to be larger, due to uncertainty in AOD, SSA and aerosol vertical profiles (Liu et al., 2019), as well as the fact that using the CP from FRESCO-S rather than deriving it here may lead to an additional error in the NO_2 AMFs. Note that these individual errors are not fully independent due to the aforementioned linkage between parameters. The magnitude of potential systematic bias in NO_2 may be smaller than the quadrature sum of errors in individual parameters, as suggested by the slight mean bias relative to MAX-DOAS data (Fig. 6a).

Table 4. Contributions of estimated errors in POMINO-TROPOMI NO_2 AMFs.

Error source		Estimated error in parameter	Corresponding error in tropospheric NO_2 AMF
NO_2 profiles			±10% [1]
Cloud fraction		±0.01 [2]	±10% [2]
Cloud pressure		±50 hPa [3]	±10% [3]
BRDF coefficients		±10% [4]	±10% [4]
Aerosol	AOD	±0.07 [5]	±10% for clean situations; Up to ±20% for heavy-polluted cases [8]
	SSA	±0.03 [6]	
	Aerosol layer height	Underestimated by 300–600 m [7]	

[1] This error estimate is based on Lin et al. (2010), Lin et al. (2014), Boersma et al. (2004, 2011, 2019) and this study. The error accounts for effect of horizontal resolutions and the vertical process in GEOS-Chem.

[2] This accounts for the expectation that our explicit aerosol correction leads to more reasonable CFs.

[3] Based on van Geffen et al. (2019). Our estimated NO_2 errors related to the use of FRESCO CP data (instead of re-calculating it) are within this error range.

[4] The estimated parameter error is taken from Zhou et al. (2010), and the corresponding AMF error is based on Lin et al. (2014) and Case 4.

[5] Based on Tian et al. (2019), who compared the MODIS Merged AOD C6.1 product with AERONET in China.

[6] Based on Lin et al. (2015), who compared GEOS-Chem simulated SSA with Lee et al. (2007).

[7] Based on Liu et al. (2019), who compared GEOS-Chem simulated aerosol extinction profiles with CALIOP.

[8] This is a tentative error estimate based on Lin et al. (2015), Lorente et al. (2017), Liu et al. (2019) and this study. With explicit aerosol corrections, the errors in heavy-polluted situations are expected to be smaller than when assuming implicit aerosol corrections.

4 Conclusion and Discussion

The POMINO algorithm to retrieve tropospheric NO_2 VCDs has been successfully applied to TROPOMI over East Asia. The resulting POMINO-TROPOMI product shows higher tropospheric NO_2 VCDs (by about 35% averaged over East Asia) and much clearer urban and other hotspot signals, compared to the TM5-MP-DOMINO (OFFLINE) product. Further evaluation using independent MAX-DOAS measurements indicates very good performance of POMINO-TROPOMI in capturing the day-to-day variation (R^2 = 0.75, N = 63) and mean value (NMB = 0.8%) of NO_2, better than TM5-MP-DOMINO (0.68 and −41.9%, respectively).

Over heavy aerosol-loaded regions, the accuracy of retrieved NO_2 VCDs is affected substantially by how aerosols are represented in the retrieval process (implicit or explicit). The implicit aerosol representation tends to underestimate the NO_2 VCDs by 0-50% over most urban areas in East Asia and by about 25% over Northern East China. Using a priori NO_2 profile data at a horizontal resolution of ~ 25 km, POMINO-TROPOMI captures the city-scale NO_2 hotspots. Reducing the horizontal resolution of a priori profiles to what is typically set up by global models (100–200 km) underestimates the NO_2 hotspots and the spatial gradient surrounding them, and the effects are more pronounced in calm than in windy situations. Overall, our results provide useful information to improve TROPOMI retrieval algorithms, and offer insight for applications to the upcoming geostationary satellite instruments including GEMS, TEMPO and Sentinel-4 Precursor.

Further work can be done to improve the retrieval algorithm for TROPOMI. The hybrid cloud retrieval method used in POMINO-TROPOMI is not optimal, because only cloud fraction but not cloud pressure is re-calculated with explicit aerosol corrections and BRDF effects. The uncertainty caused by inconsistent assumptions of aerosols and albedos in cloud pressure and NO_2 VCD retrievals are initially estimated in this study. Re-calculation of cloud pressure will be done in the future using the O_2-O_2 method when the O_2-O_2 SCD data are available. Second, correcting the simulated aerosol extinction vertical profiles will further improve the clouds and NO_2 retrievals (Liu et al., 2019). Third, the horizontal resolution of a priori NO_2 profiles (~ 25 km) does not match the fine footprint of TROPOMI, and further increasing the resolution will help achieve better accuracy for analyses of very fine scale pollution characteristics such as along the highways and rivers and within urban centers.

Acknowledgments

Acknowledgements. This study is supported by the National Natural Science Foundation of China (41775115) and Ministry of Science and Technology (2019QZKK0604).

Data availability. The POMINO-TROPOMI NO_2 data are available at our website (http://www.pku-atmos-acm.org/acmProduct.php/). The TM5-MP-DOMINO product can be download via TEMIS website: http://www.temis.nl/airpollution/no2.html. The near surface data of NO_2 and $PM_{2.5}$ can be downloaded from: http://www.cnemc.cn/sssj/cskqzl/. The ground-based MAX-DOAS observations would be provided after the applications of users are approved by corresponding owners.

Author contributions. J.-T. Lin conceived the research. M.-Y. Liu and J.-T. Lin designed the experiment. M.-Y. Liu performed all calculations with some code support from H. Kong and H.-J. Weng. M.-Y. Liu and J.-T. Lin wrote the paper with inputs from K.-F. Boersma and J.-H. Eske. R. Spurr provided LIDORT. Y. Kanaya, Q. He, X. Tian, K. Qin, P.-H. Xie provided the MAX-DOAS observations. R.-J. Ni helped to process surface observations. Y.-Y. Yan and J.-X. Wang helped to analyze the relationship between meteorological and NO_2 VCD variations. All authors commented on the manuscript.

Competing interests. The authors declare no conflicts of interest.

References

Arnoud, A., Mattia, P., Maarten, S., Veefkind, J. P., Loyola, D., & Wang, P. (2017). *Sentinel-5 precursor/TROPOMI Level 2 Product User Manual KNMI level 2 support products*. Retrieved from De Bilt, the Netherlands: https://sentinel.esa.int/documents/247904/2474726/Sentinel-5P-Level-2-Product-User-Manual-FRESCO-Cloud-Support

Boersma, K. F., Eskes, H. J., & Brinksma, E. J. (2004). Error analysis for tropospheric NO_2 retrieval from space. *Journal of Geophysical Research: Atmospheres, 109*(D4). doi:10.1029/2003JD003962

Boersma, K. F., Eskes, H. J., Dirksen, R. J., van der A, R. J., Veefkind, J. P., Stammes, P., Brunner, D. (2011). An improved tropospheric NO_2 column retrieval algorithm for the Ozone Monitoring Instrument. *Atmos. Meas. Tech., 4*(9), 1905-1928. doi:10.5194/amt-4-1905-2011

Boersma, K. F., Eskes, H. J., Richter, A., De Smedt, I., Lorente, A., Beirle, S., Compernolle, S. C. (2018). Improving algorithms and uncertainty estimates for satellite NO_2 retrievals: results from the quality assurance for the essential climate variables (QA4ECV) project. *Atmos. Meas. Tech., 11*(12), 6651-6678. doi:10.5194/amt-11-6651-2018

Dentener, F., van Weele, M., Krol, M., Houweling, S., & van Velthoven, P. (2003). Trends and inter-annual variability of methane emissions derived from 1979-1993 global CTM simulations. *Atmos. Chem. Phys., 3*(1), 73-88. doi:10.5194/acp-3-73-2003

Eskes, H., van Geffen, J. H. G. M., Boersma, F., Sneep, M., ter Linden, M., & Veefkind, P. (2018). *Sentinel-5P TROPOMI high-resolution nitrogen dioxide observations.* Paper presented at the American Geophysical Union Fall Meeting, Walter E Washington Convention Center, Washington, D.C.

Eskes, H. J., Eichmann, K. U., Lambert, J. C., Loyola, D., Veefkind, J. P., Dehn, A., & Zehner, C. (2019). *S5P Mission Performance Centre Nitrogen Dioxide [L2__NO2___] Readme* (01.03.00). Retrieved from De Bilt, the Netherlands: https://sentinel.esa.int/documents/247904/3541451/Sentinel-5P-Nitrogen-Dioxide-Level-2-Product-Readme-File

Goryl, P., Zehner, C., & Laur, H. (2017). *Sentinel-5 Precursor Calibration and Validation Plan for the Operational Phase*. Retrieved from De Bilt, the Netherlands: https://sentinel.esa.int/documents/247904/2474724/Sentinel-5P-Calibration-and-Validation-Plan.pdf

Griffin, D., Zhao, X., McLinden, C. A., Boersma, F., Bourassa, A., Dammers, E., Wolde, M. (2019). High-Resolution Mapping of Nitrogen Dioxide With TROPOMI: First Results and Validation Over the Canadian Oil Sands. *Geophysical Research Letters, 46*(2), 1049-1060. doi:10.1029/2018gl081095

Hoek, G., Krishnan, R. M., Beelen, R., Peters, A., Ostro, B., Brunekreef, B., & Kaufman, J. D. (2013). Long-term air pollution exposure and cardio- respiratory mortality: a review. *Environmental Health, 12*(1), 43. doi:10.1186/1476-069x-12-43

Kanaya, Y., Irie, H., Takashima, H., Iwabuchi, H., Akimoto, H., Sudo, K., Panchenko, M. (2014). Long-term MAX-DOAS network observations of NO_2 in Russia and Asia (MADRAS) during the period 2007-2012: instrumentation, elucidation of climatology, and comparisons with OMI satellite observations and global model simulations. *Atmos. Chem. Phys., 14*(15), 7909-7927. doi:10.5194/acp-14-7909-2014

Kleipool, Q. L., Dobber, M. R., de Haan, J. F., and Levelt, P. F. (2008), Earth surface reflectance climatology from 3 years of OMI data, J. Geophys. Res., 113, D18308, doi:10.1029/2008JD010290.

Krotkov, N. A., McLinden, C. A., Li, C., Lamsal, L. N., Celarier, E. A., Marchenko, S. V., Streets, D. G. (2016). Aura OMI observations of regional SO_2 and NO_2 pollution changes from 2005 to 2015. *Atmos. Chem. Phys., 16*(7), 4605-4629. doi:10.5194/acp-16-4605-2016

Laughner, J. L., Zare, A., & Cohen, R. C. (2016). Effects of daily meteorology on the interpretation of space-based remote sensing of NO_2. *Atmos. Chem. Phys., 16*(23), 15247-15264. doi:10.5194/acp-16-15247-2016

Lee, K. H., Li, Z., Wong, M. S., Xin, J., Wang, Y., Hao, W. M., and Zhao, F.: Aerosol single scattering albedo estimated across China from a combination of ground and satellite measurements, J. Geophys. Res., 112, D22S15, doi:10.1029/2007JD009077, 2007

Lin, J., & Li, J. (2016). Spatio-temporal variability of aerosols over East China inferred by merged visibility-GEOS-Chem aerosol optical depth. *Atmospheric Environment, 132*, 111-122. doi:https://doi.org/10.1016/j.atmosenv.2016.02.037

Lin, J. T., Liu, M. Y., Xin, J. Y., Boersma, K. F., Spurr, R., Martin, R., & Zhang, Q. (2015). Influence of aerosols and surface reflectance on satellite NO_2 retrieval: seasonal and spatial characteristics and implications for NO_x emission constraints. *Atmos. Chem. Phys., 15*(19), 11217-11241. doi:10.5194/acp-15-11217-2015

Lin, J. T., Martin, R. V., Boersma, K. F., Sneep, M., Stammes, P., Spurr, R., Irie, H. (2014). Retrieving tropospheric nitrogen dioxide from the Ozone Monitoring Instrument: effects of aerosols, surface reflectance anisotropy, and vertical profile of nitrogen dioxide. *Atmos. Chem. Phys., 14*(3), 1441-1461. doi:10.5194/acp-14-1441-2014

Lin, J. T., McElroy, M. B., & Boersma, K. F. (2010). Constraint of anthropogenic NO_x emissions in China from different sectors: a new methodology using multiple satellite retrievals. *Atmos. Chem. Phys., 10*(1), 63-78. doi:10.5194/acp-10-63-2010

Liu, M., Lin, J., Boersma, K. F., Pinardi, G., Wang, Y., Chimot, J., Ni, R. (2019). Improved aerosol correction for OMI tropospheric NO_2 retrieval over East Asia: constraint from CALIOP aerosol vertical profile. *Atmos. Meas. Tech., 12*(1), 1-21. doi:10.5194/amt-12-1-2019

Lorente, A., Folkert Boersma, K., Yu, H., Dörner, S., Hilboll, A., Richter, A., . . . Krol, M. (2017). Structural uncertainty in air mass factor calculation for NO_2 and HCHO satellite retrievals. *Atmos. Meas. Tech., 10*(3), 759-782. doi:10.5194/amt-10-759-2017

Maasakkers, J. D., K. F. Boersma, J. E. Williams, J. Van Geffen, G. C. M. Vinken, M. Sneep, F. Hendrick, M. Van Roozendael, and J. P. Veefkind (2013), Vital improvements to the retrieval of tropospheric NO2 columns from the Ozone Monitoring Instrument, in EGU General Assembly 2013, edited, pp. EGU2013-2714, EGU General Assembly Conference Abstracts.

McLinden, C. A., Fioletov, V., Boersma, K. F., Kharol, S. K., Krotkov, N., Lamsal, L., Yang, K. (2014). Improved satellite retrievals of NO_2 and SO_2 over the Canadian oil sands and comparisons with surface measurements. *Atmos. Chem. Phys., 14*(7), 3637-3656. doi:10.5194/acp-14-3637-2014

Ott, L. E., Pickering, K. E., Stenchikov, G. L., Allen, D. J., DeCaria, A. J., Ridley, B., Tao, W.-K. (2010). Production of lightning NO_x and its vertical distribution calculated from three-dimensional cloud-scale chemical transport model simulations. *Journal of Geophysical Research: Atmospheres, 115*(D4). doi:doi:10.1029/2009JD011880

Russell, A. R., Perring, A. E., Valin, L. C., Bucsela, E. J., Browne, E. C., Wooldridge, P. J., & Cohen, R. C. (2011). A high spatial resolution retrieval of NO_2 column densities from OMI: method and evaluation. *Atmos. Chem. Phys., 11*(16), 8543-8554. doi:10.5194/acp-11-8543-2011

Shindell, D. T., Faluvegi, G., Koch, D. M., Schmidt, G. A., Unger, N., & Bauer, S. E. (2009). Improved Attribution of Climate Forcing to Emissions. *Science, 326*(5953), 716-718. doi:10.1126/science.1174760

Tian, X., P. Xie, J. Xu, A. Li, Y. Wang, M. Qin, and Z. Hu (2018), Long-term observations of tropospheric NO_2, SO_2 and HCHO by MAX-DOAS in Yangtze River Delta area, China, Journal of Environmental Sciences, 71, 207-221. doi:10.1016/j.jes.2018.03.006

van Geffen, J. H. G. M., Eskes, H. J., Boersma, K. F., Maasakkers, J. D., & Veefkind, J. P. (2019). *TROPOMI ATBD of the total and tropospheric NO_2 data products (issue 1.4.0)*. Retrieved from De Bilt, the Netherlands: https://sentinel.esa.int/documents/247904/2476257/Sentinel-5P-TROPOMI-ATBD-NO2-data-products

Veefkind, J. P., Aben, I., McMullan, K., Förster, H., de Vries, J., Otter, G., . . . Levelt, P. F. (2012). TROPOMI on the ESA Sentinel-5 Precursor: A GMES mission for global observations of the atmospheric composition for climate, air quality and ozone layer applications. *Remote Sensing of Environment, 120*, 70-83. doi:https://doi.org/10.1016/j.rse.2011.09.027

Wang, Y., Lampel, J., Xie, P., Beirle, S., Li, A., Wu, D., & Wagner, T. (2017). Ground-based MAX-DOAS observations of tropospheric aerosols, NO_2, SO_2 and HCHO in Wuxi, China, from 2011 to 2014. *Atmos. Chem. Phys., 17*(3), 2189-2215. doi:10.5194/acp-17-2189-2017

Williams, J. E., Boersma, K. F., Le Sager, P., & Verstraeten, W. W. (2017). The high-resolution version of TM5-MP for optimized satellite retrievals: description and validation. *Geosci. Model Dev., 10*(2), 721-750. doi:10.5194/gmd-10-721-2017

Zara, M., Boersma, K. F., De Smedt, I., Richter, A., Peters, E., van Geffen, J. H. G. M., Eskes, H. J. (2018). Improved slant column density retrieval of nitrogen dioxide and formaldehyde for OMI and GOME-2A from QA4ECV: intercomparison, uncertainty characterisation, and trends. *Atmos. Meas. Tech., 11*(7), 4033-4058. doi:10.5194/amt-11-4033-2018

Zhou, Y., D. Brunner, R. J. D. Spurr, K. F. Boersma, M. Sneep, C. Popp, and B. Buchmann (2010), Accounting for surface reflectance anisotropy in satellite retrievals of tropospheric NO_2, Atmos. Meas. Tech., 3(5), 1185-1203.